

- Wakes," paper presented at Fourth Austral. Conf. on Hydraulics and Fluid Mechanics, Melbourne (1971).
- Kozeny, J., "Über Kapillare Leitung des Wassers im Boden," *Ber. Wien, Akd.*, **136**, 271 (1927).
- Kusik, C. L., and J. Happel, "Boundary Layer Mass Transport with Heterogeneous Catalysis," *AIChE J.*, **8**, 163 (1962).
- Kyle, C. R., and R. L. Perrine, "An Experimental Model of Visual Studies of Turbulent Flow in Porous Materials," *Can. J. Chem. Eng.*, **49**, 19 (1971).
- Leva, Max, "Pressure Drop through Packed Tubes: Part I. A General Correlation," *Chem. Eng. Progr.*, **43**, 713 (1947).
- Martin, J. J., W. L. McCabe, and C. C. Monrad, "Pressure Drop Through Stacked Spheres: Effect of Orientation," *ibid.*, **47**, 91 (1951).
- Oman, A. O., and K. M. Watson, "Pressure Drops in Granular Beds," *Refinery Mat. Petrol. Chem. Tech.*, **36**, R795 (1944).
- Pasternak, I. S., and W. H. Gauvin, "Turbulent Convective Heat and Mass Transfer From Accelerating Particles," *AIChE J.*, **7**, 254 (1961).
- Price, J., "Velocity Distribution and Pressure Losses for Randomly Packed Beds of Spheres," Australian Atomic Energy Comm. Rep. AAEC/E178 (1967).
- , "The Distribution of Fluid Velocities for Randomly Packed Beds of Spheres," *Mech. Chem. Eng. Trans., Instrn. Engrs., Australia*, **7** (1968).
- Ranz, W. E., "Friction and Transfer Coefficients for Single Particles and Packed Beds," *Chem. Eng. Progr.*, **48**, 247 (1952).
- Scheidegger, A. E., *The Physics of Flow through Porous Media*, MacMillan, New York (1961).
- Standish, N., and J. B. Drinkwater, "The Effect of Particle Shape on Flooding Rates in Packed Columns," *Chem. Eng. Sci.*, **25**, 1619 (1970).
- Stanek, V., and J. Szekely, "The Effect of Non-Uniform Porosity in Causing Flow Maldistributions in Isothermal Packed Beds," *Can. J. Chem. Eng.*, **50**, 9 (1972).
- Van der Merwe, D. F., and W. H. Gauvin, "Pressure Drag Measurements for Turbulent Air Flow Through a Packed Bed," *AIChE J.*, **17**, 402 (1971a).
- , "Velocity and Turbulence Measurements of Air Flow Through a Packed Bed," *ibid.*, 519 (1971b).
- Wentz, Jr., C. A., and G. Thodos, "Pressure Drops in the Flow of Gases Through Packed and Distended Beds of Spherical Particles," *AIChE J.*, **9**, 81 (1963).

Manuscript received December 18, 1972; revision received and accepted March 9, 1972.

Thermodynamic Properties of Supercritical Fluids and their Mixtures at Very High Pressures

Experimental and estimated PVT data for simple fluids at very high pressures have been correlated with corresponding states theory. Generalized tables and charts are given for density, enthalpy, fugacity, and internal energy for the reduced temperature range 1 to 50 and for reduced pressures to 2000. Consideration is given to possible solidification at very high pressures and to applicability of the reduced charts to quantum fluids, water and ammonia, through temperature-dependent effective critical constants. The van der Waals two-fluid model of binary mixtures is used to calculate properties of mixtures including the composition of coexisting phases. The correlations presented here are useful for estimating thermodynamic properties at very high pressures.

GERRIT J. F. BREEDVELD
and
JOHN M. PRAUSNITZ

Chemical Engineering Department
University of California
Berkeley, California 94720

SCOPE

In chemical technology there are many important processes which are performed at high pressures. Common examples include the synthesis of ammonia and the synthesis of methanol operating at pressures near 500 atm and the polymerization of ethylene to yield low-density polyethylene, operating at pressures near 3000 atm. In the future it is likely that new processes will be developed at still higher pressures than those in common use today. Rational design of chemical reactors and separation operations at high pressures requires thermodynamic

properties of fluids at these pressures. For simple fluids such properties can be estimated with good accuracy from existing corresponding-states correlations. These correlations, however, go to a reduced pressure of 100 at the most. Therefore, for estimating thermodynamic properties of simple fluids and their mixtures at much higher pressures, a corresponding-states correlation was prepared covering reduced pressures from 1 to 2000 and reduced temperatures from 1 to 50. This correlation is presented in the form of generalized tables and charts.

CONCLUSIONS AND SIGNIFICANCE

In anticipation of future developments in high pressure chemical technology, we have extended the existing corresponding-states correlations to enable the estimation of the thermodynamic properties of simple fluids at reduced pressures up to 2000 and reduced temperatures up to 50. Generalized charts and tables are given for density, enthalpy, fugacity, and internal energy.* The correlations were extended to include quantum fluids and polar substances (ammonia and water) through introduction of effective temperature-dependent critical parameters. Spe-

cial attention is given to possible solidification at very high pressures. The van der Waals two-fluid model, in conjunction with these charts and tables, is used for calculating thermodynamic properties of several binary mixtures including the composition of co-existing phases (gas-gas equilibria). The charts and tables are useful for estimating thermodynamic properties of supercritical simple fluids and their mixtures at high pressures. They may be of assistance in exploratory research and in engineering work where experimental data are scarce.

For design of chemical processes and chemical process equipment at high pressures, it is often necessary to estimate the configurational properties of fluids. In many cases these estimates can be made using empirical equations of state, generalized tables, or charts based on the theorem of corresponding states as discussed in numerous references (see, for example, Dodge, 1944; Hougen et al., 1964; Leland and Chappelaar, 1968; Lewis et al., 1961). However, these equations and charts represent experimental data over only a limited range of pressures and temperatures. The well-known tables of Pitzer et al. (see Lewis et al., 1961) give generalized results for reduced temperatures T_R up to 4 and for reduced pressures P_R up to 9; the tables of Hougen et al. (1964) have as their upper limits a reduced temperature of 15 and a reduced pressure of 30, while the older charts presented by Dodge (1944) go to $T_R = 35$ and at the most a reduced pressure of 100. For present day applications these upper limits are satisfactory since few chemical or physical processes are operated at conditions exceeding these limits, but in the near future new processes may well be proposed (see, for example, Gonikberg, 1960; Schneider, 1970; Weale, 1967), which will require appreciably higher temperatures and/or pressures. To evaluate critically the technical feasibility of such processes it will be necessary to calculate densities, fugacities, entropies, enthalpies and energies of the fluids concerned.

We present here generalized charts covering a reduced pressure range up to 2000 and a reduced temperature range between 1 and 50. More detailed information in tabular form is given elsewhere (Breedveld, 1972).

GENERALIZED DENSITY CHART

Only a few authors have reported experimental PVT data for simple supercritical fluids at high pressures (exceeding 1000 atm), but these data coupled with rational interpolations and extrapolations are sufficient to give a generalized representation. Sources of PVT data are given in Table 1. Detailed information concerning construction of the tables and graphs is presented elsewhere (Breedveld, 1972). Three equations of state were helpful in providing guidance for interpolation, extrapolation, and smoothing of the data. These are the Tait equation (Tait, 1899, 1900; Tsiklis, 1951, 1953), the Strohbridge-Gosman equation (Gosman et al., 1969; Preston and Frausnitz, 1971), and the Harrison equation (Harrison, 1964). At high densities (more than twice the critical density) the PVT properties of fluids are well represented by the Tait

equation and we have used this equation to calculate densities five to six times the critical. The Strohbridge-Gosman equation proved useful in the reduced temperature range 1 to 2 and the reduced pressure range from 1 to about 150. The Harrison equation served well in the reduced temperature range of 22 to 50 and the reduced pressure range from 1 to 900.

The resultant data were plotted on reduced coordinates as shown in Figure 1 where the reduced density ρ_R is shown as a function of reduced pressure with reduced temperature as parameter. A crossplot of Figure 1 is shown in Figure 2 where reduced density is given as a function of reduced temperature with reduced pressure as parameter.

For the classical fluids the reducing parameters used were the experimental critical properties. For the quantum fluids (helium, hydrogen, neon), temperature-dependent, effective critical constants were given by Gunn et al. (1966; see also Table 2). The results shown in Figures 1 and 2 represent smoothed, reduced densities and are also given in a more detailed table elsewhere (Breedveld, 1972). Table 3 gives an indication of the expected accuracy. At modest reduced temperatures and pressures our charts agree well with Pitzer's tables for an acentric factor ω near 0.02, with deviations varying roughly between -2 and $+2\%$. Table 3a, covering a reduced temperature range from 1 to 44 and a reduced pressure range from 4 to 400, shows deviations of the same magnitude. At very high reduced pressures (500 to 1600) and at reduced temperatures varying from 13 to 16, the generalized densities are in good agreement with results of shockwave experiments on argon reported by Keeler et al. (1965),

TABLE 1. SOURCES OF EXPERIMENTAL PVT DATA AT HIGH PRESSURES

Fluid	Temperature range, °K	Highest pressure, atm	References
Argon	150.7-5000	14,500	a, b, c, d, e
Nitrogen	126.3-3000	14,500	a, f, c, g, h
Helium	13.5-473	14,500	a, i, j, k, l
Hydrogen	100.0-423	12,600	a, m, j, n, o
Neon	130.0-423	2,900	p, q
Xenon	298.0-423	2,800	r
Carbon monoxide	225.0-532	1,200	s
Methane	229.0-439	1,000	f

a. Bridgman, 1924; b. Din, vol. 2, 1956; c. Hilsenrath et al., 1960; d. Michels et al., 1949; e. Polyakov et al., 1967; f. Din, vol. 3, 1961; g. Strohbridge, 1962; h. Tsiklis, 1951; i. Buchmann, 1933; j. Holley et al., 1958; k. Sullivan and Sonntag, 1967; l. Wiebe et al., 1931; m. Goodwin et al., 1962; n. Michels and Goudekot, 1941; o. Perry, 1963; p. Michels et al., 1960; q. Streett, 1971; r. Michels et al., 1954; s. Din, vol. 1, 1956.

* A Supplement containing detailed tables and additional information on their constructions, accuracy, and uses has been deposited as Document No. 02105 with National Auxiliary Publications Service (NAPS), c/o Microfiche Publications, 345 E. 46 St., New York, N. Y. 10017 and may be obtained for \$1.50 for microfiche and \$8.45 for photocopies.

Ross and Alder (1967), and Ross (1968), with accuracies varying between - 1 to - 8%.

GENERALIZED FUGACITY AND ENTHALPY CHARTS

Using standard thermodynamic relations, the generalized density data were integrated isothermally with respect to pressure to obtain fugacities; these fugacities were differentiated with respect to temperature to obtain enthalpy departures from the ideal-gas values. Final results were adjusted slightly to improve agreement with experi-

mental enthalpies and fugacities and to assure thermodynamic consistency. Tables 3b and 3c give a rough idea of the expected accuracies for reduced temperatures up to 12 and reduced pressures up to 300. These accuracies (averages of the absolute values of the % deviation) vary from 2 to 6 for the fugacities and from 4 to 8 for the enthalpies, and thus are generally lower than those for the densities. This matter is discussed in more detail elsewhere (Breedveld, 1972).

Figure 3 shows fugacity coefficients f/P . The values of f/P become very large as the pressure rises. At a reduced temperature of unity and a reduced pressure equal to two thousand, the ratio of fugacity to pressure is 10^{49} .

From Figures 4 and 5, which show reduced enthalpy departures $\Delta H/RT_c$, where $\Delta H = H(O, T) - H(P, T)$, it is apparent that at high reduced pressures ΔH is negative. At such pressures, contrary to the behavior of fluids at normal conditions, isothermal vaporization (increasing the

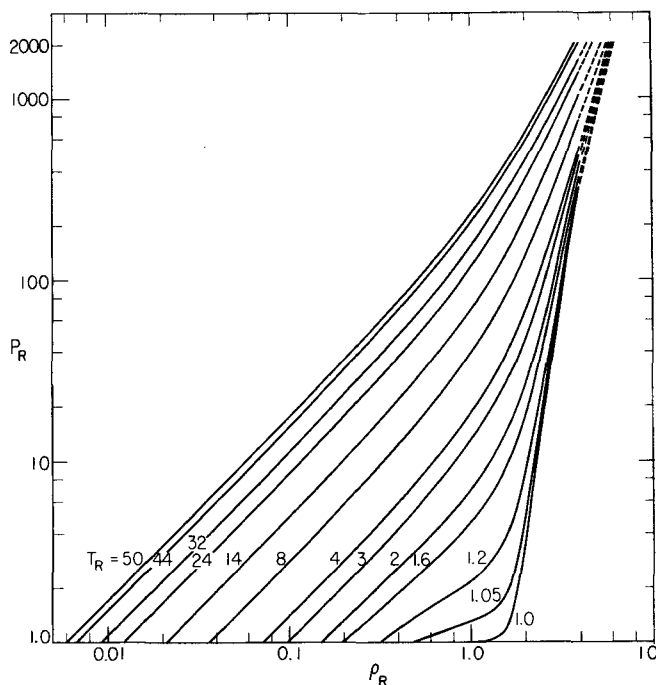


Fig. 1. Generalized reduced densities at very high pressures (isotherms).

TABLE 2. DATA FOR CALCULATING TEMPERATURE-DEPENDENT EFFECTIVE CRITICAL CONSTANTS OF QUANTUM FLUIDS (GUNN ET AL., 1966)

$$T_c^* = \frac{T_c^\circ}{1 + \frac{C_1}{MT}}; P_c^* = \frac{P_c^\circ}{1 + \frac{C_2}{MT}};$$

$$V_c^* = \frac{0.292RT_c^*}{P_c^*} = \frac{V_c^\circ}{1 + \frac{C_3}{MT}}.$$

$C_1 = 21.8^\circ\text{K}$; $C_2 = 44.2^\circ\text{K}$; C_3 is determined from P_c^* , T_c^* and V_c^* .

	$T_c^*, ^\circ\text{K}$	P_c^*, atm	$V_c^*, \text{cm}^3\text{mole}^{-1}$
Hydrogen	43.6	20.2	51.5
Helium ($M=4$)	10.47	6.67	37.5
Neon	45.5	26.9	40.3

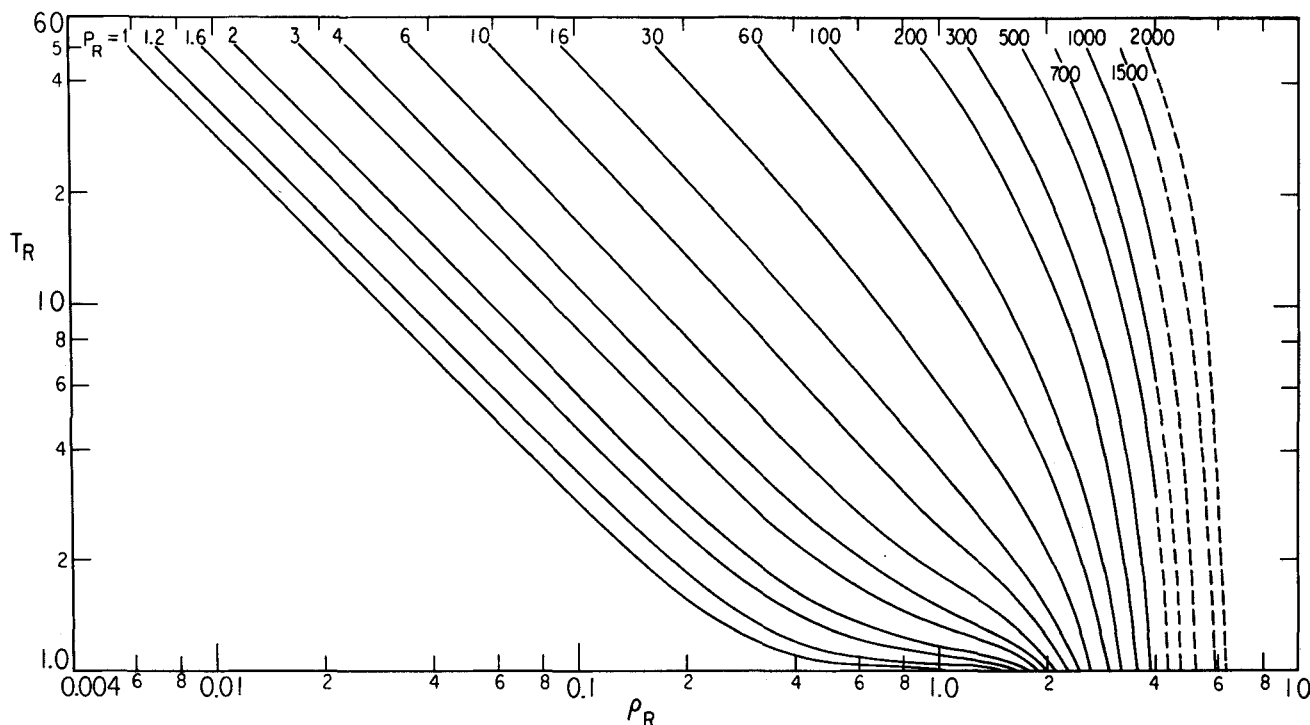


Fig. 2. Generalized reduced densities at very high pressures (isobars).

volume) is accompanied by a loss, rather than a gain, of enthalpy. For example, if argon at 660°K is compressed to 48,000 atm and then vaporized isothermally to the ideal-gas state, the enthalpy decrease is 19,900 cal/mole. (For comparison, the enthalpy increase upon vaporization of argon at its normal boiling point is 1560 cal/mole.) If argon at 660°K and 48,000 atm is throttled to low pressure in a constant-enthalpy (Joule-Thomson) process, its temperature rises to 4670°K. Detailed tabulated results represented by Figures 3, 4, and 5 are given elsewhere (Breedveld, 1972).

The entropy difference, relative to an ideal gas at the same pressure and temperature, can be found readily from Figures 3 and 4 (or 5) by standard thermodynamics.

Figures 1 and 4 (or 5) were used to calculate $U(O, T)$

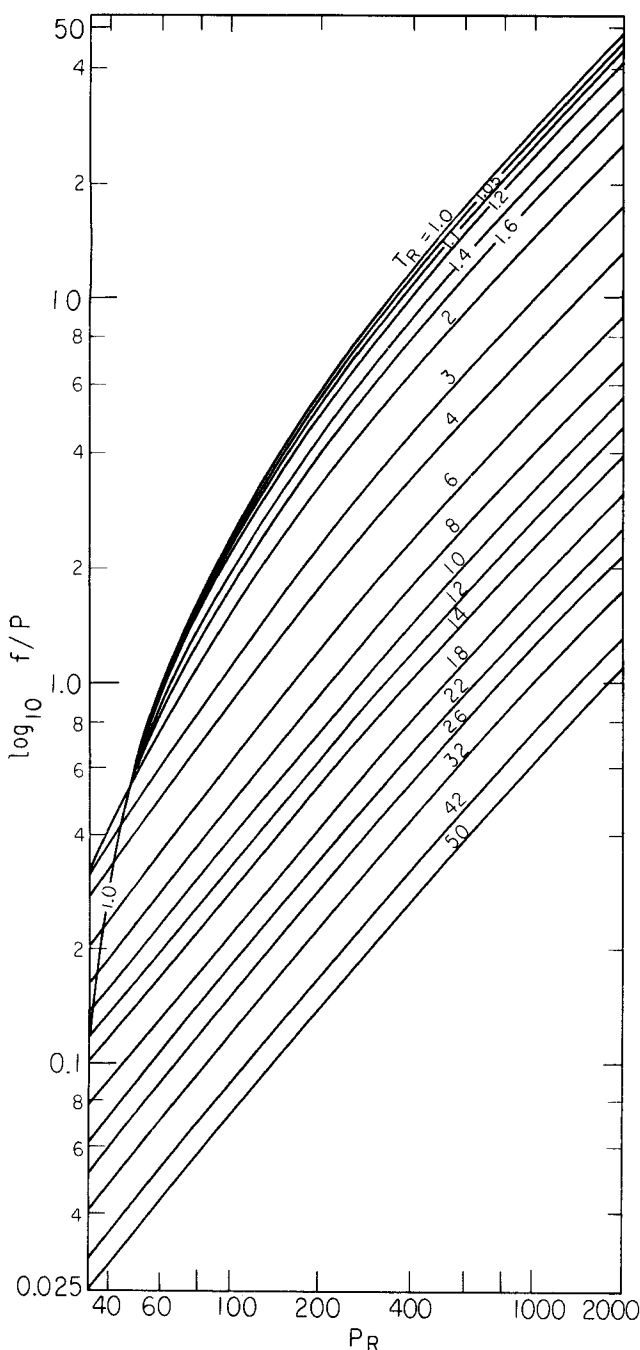


Fig. 3. Generalized fugacity coefficients at very high pressures (isotherms).

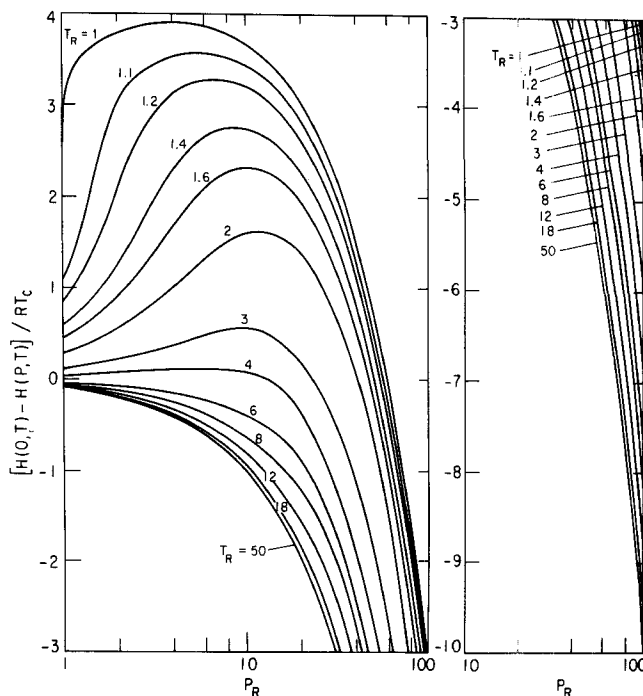


Fig. 4. Generalized enthalpy differences at very high pressures (isotherms).

TABLE 3A. ESTIMATED ACCURACY IN REDUCED DENSITY FOR SIMPLE FLUIDS

Temperature range, °K	Pressure range, atm	Accuracy %	Reference
Nitrogen 130.0-600.0	300-10,000	0.5-1.8	a
Argon 160.0-500.0	300-3,000	0.9-3.4	b
Hydrogen 273.2-423.2	210-3,700	1.6-1.9	c
Helium 70.0-120.0	50-700	0.7-2.0	d

a. Din, vol. 3, 1961; b. Din, vol. 2, 1956; c. Michels and Goudek, 1941; d. Sullivan and Sonntag, 1967.

TABLE 3B. ESTIMATED ACCURACY IN FUGACITY COEFFICIENTS FOR SIMPLE FLUIDS

Range T_R	Range P_R	Range $\log_{10} f/P^\dagger$	Accuracy* %	Reference
1.3 to 12.0	4.2 to 126	0.1 to 0.5	6	a,b,c,d,e
1.3 to 10.0	9 to 193	>0.5 to 1.0	2	a,b,c,d,e
1.0 to 3.0	90 to 298	>1.0 to 4.0	2	a,b,c

† Absolute values.

* Average of absolute values of % deviation from reference data.

a. Din, vol. 3, 1961; b. Din, vol. 2, 1956; c. Michels et al., 1949; d. Michels and Goudek, 1941; e. Sullivan and Sonntag, 1967.

TABLE 3C. ESTIMATED ACCURACY IN ENTHALPY DIFFERENCES FOR SIMPLE FLUIDS

Range T_R	Range P_R	Range $\Delta H/RT_c^\dagger$	Accuracy* %	Reference
1.3 to 3.0	6.3 to 59.5	0.5 to 1.0	8	a,b
1.0 to 4.8	6.3 to 103	>1.0 to 5.0	7	a,b
1.5 to 3.0	9.0 to 298	>5.0 to 20	4	a,b

† Absolute values.

* Average of absolute values of % deviation from reference data.

a. Din, vol. 3, 1961; b. Din, vol. 2, 1956.

– $U(P, T)$, the internal energy difference, by

$$U(O, T) - U(P, T) = \Delta U$$

$$= [H(O, T) - H(P, T)] - [RT - PV] \quad (1)$$

Results are shown in Figures 6 and 7.

The use of these charts in conjunction with the Scatchard-Hildebrand theory of regular solutions (Hildebrand et al., 1970) is discussed in Appendix I.

APPLICATION OF GENERALIZED CHARTS TO WATER AND TO AMMONIA

Because of their large importance in chemical technology, it is desirable that the generalized charts be applicable to water and to ammonia; this is particularly important when we want to estimate properties of mixtures containing either water or ammonia as one of the components. Water and ammonia are strongly polar and therefore configurational properties are not represented by simple corresponding-states correlations. However, Rowlinson (p. 275, 1969), Prigogine (Ch. 14, 1957), Danon and Amdur (1969), and others (Bae and Reed, 1967; Cook and Rowlinson, 1953) have shown that at temperatures well above the normal boiling point the configurational properties of simple polar fluids can be superim-

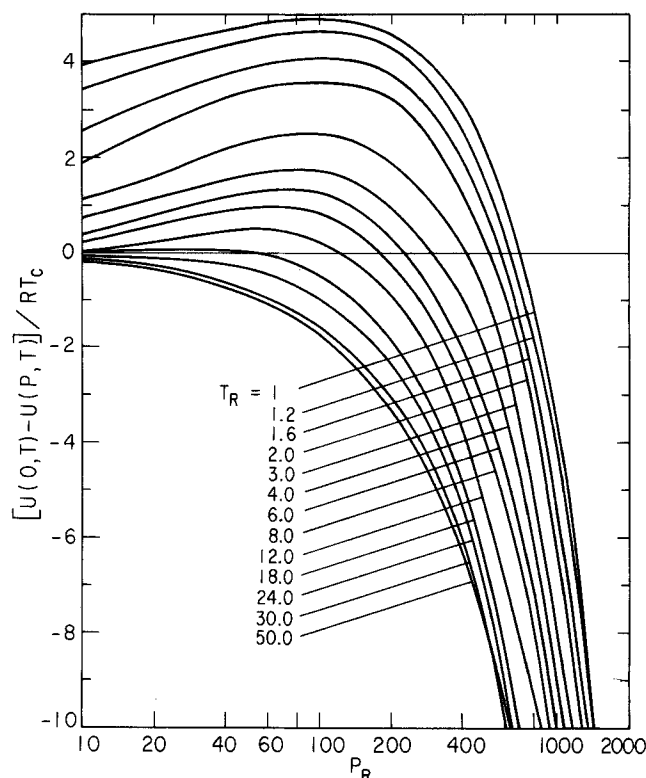


Fig. 6. Generalized energy differences at very high pressures (isotherms).

TABLE 4. EFFECTIVE CRITICAL CONSTANTS FOR SUPERCRITICAL WATER^a

$T, ^\circ\text{K}$	P_c^*, atm	$T_c^*, ^\circ\text{K}$
693.2	327.4	705.5
713.2	326.3	701.6
873.2	316.3	670.1
1,073.2	299.5	623.0

^a. Obtained from fit to experimental f/P values in the range 100-5000 atm.

TABLE 5. EFFECTIVE CRITICAL CONSTANTS FOR SUPERCRITICAL AMMONIA^a

$T, ^\circ\text{K}$	P_c^*, atm	$T_c^*, ^\circ\text{K}$
420	157.9	427.4
440	154.5	427.4
560	147.5	418.3

^a. Obtained from fit to experimental f/P values in the range 1,500 to 15,000 atm.

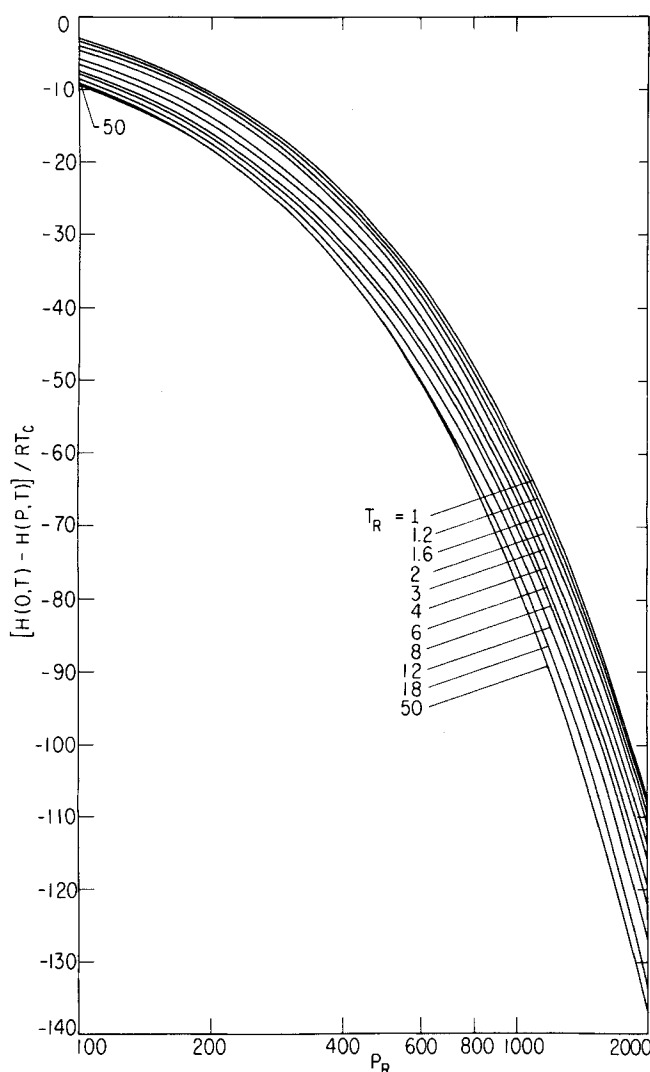


Fig. 5. Generalized enthalpy differences at very high pressures (isotherms).

posed on those of simple nonpolar fluids by using effective critical properties P_c^* and T_c^* which, to a good approximation, are linear functions of the reciprocal temperature. Effective critical constants for water are given in Table 4. These were obtained by fitting experimental f/P data for water to the generalized results. Figure 8 compares experimental values of f/P for water (Burnham et al., 1969) with those calculated. Figure 8 also shows results obtained when true critical constants, rather than the effective ones, were used in the calculations. Similar results for ammonia are shown in Figure 9 and Table 5. The Tait equation of state (Tsiklis, 1953) was used for the extrapo-

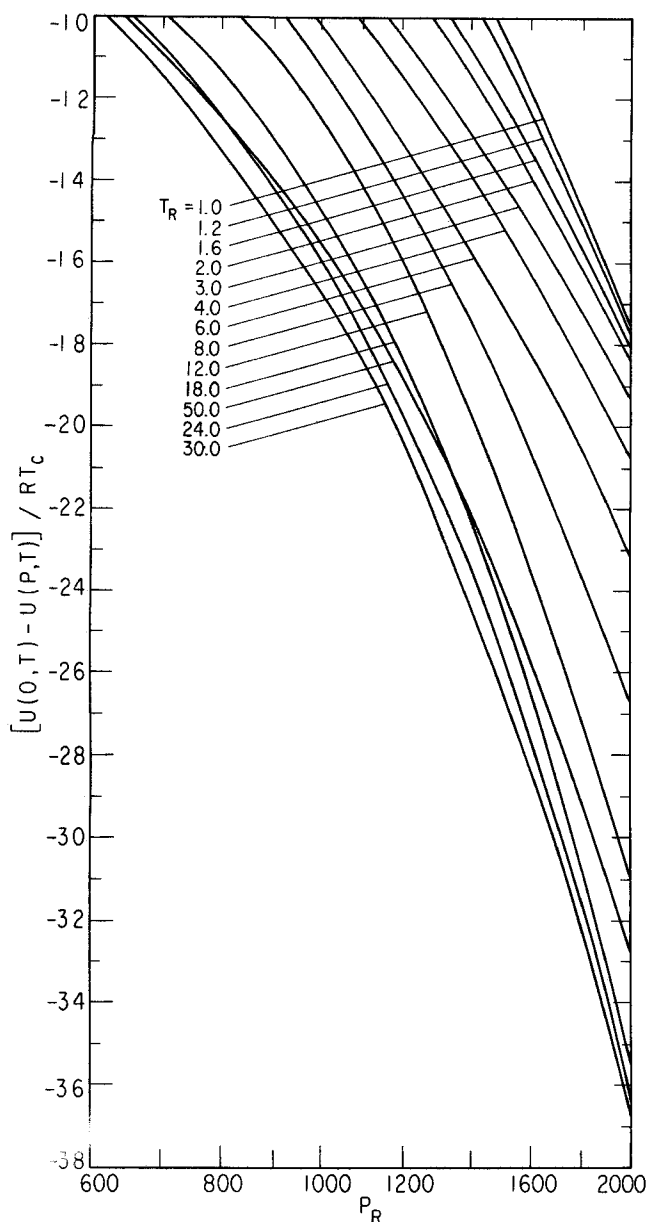


Fig. 7. Generalized energy differences at very high pressures (isotherms).

lation of existing data into the high pressure area shown in Figure 9.

EFFECT OF PRESSURE ON FREEZING

Since simple nonpolar fluids expand upon melting, the Clapeyron equation tells us that the freezing temperatures rise with increasing pressure. For noble gases experimental freezing temperatures at high pressures are well represented by the Simon equation (Holland et al., 1951; Simon, 1929):

$$\frac{P_m}{P_0} = \left(\frac{T_m}{T_0} \right)^d - 1 \quad (2)$$

where T_m is the melting temperature at pressure P_m , and P_0 , T_0 , and d are constants.

Figure 10 shows a reduced plot of the Simon equation (based on data for argon) as well as some experimental freezing temperatures for nitrogen.

When the coordinates of the Simon equation are plotted on the reduced density diagram shown in Figure 1, we obtain Figure 11 which indicates the possible region

where the supercritical fluid may have solidified. One must, therefore, never ignore the possibility of crossing the freezing curve when making calculations at very high pressures. (See, for example, Rice and Walsh, 1957.) Also, due attention should be paid to the possibility of solid-phase transitions in the P-T region of interest.

As indicated by Figure 10, the freezing line for nitrogen, a more complex molecule than the noble gases, is shifted to higher reduced densities. We have also found that the freezing points of methane, carbon dioxide, and carbon tetrachloride lie above the freezing line of argon. For water and ice VII, experimental data suggest that above but close to the critical temperature the freezing lines also lie above the freezing line of noble gases. Therefore it is likely that in many cases the dashed line of Figure 11 should be shifted to the right. This is probably the case for many fluid mixtures where freezing often occurs at temperatures well below the freezing point of either pure component. Here again it should be ascertained which solid phase is likely to exist under the conditions of interest. It is clear, however, that even if the substance in question has solidified, the tables can still be used for calculating the (hypothetical) values of thermodynamic properties of subcooled fluids.

Since the generalized tables cover a wide range of pressures and temperatures, caution must be exercised in their use in order to avoid errors due to ionization, dis-

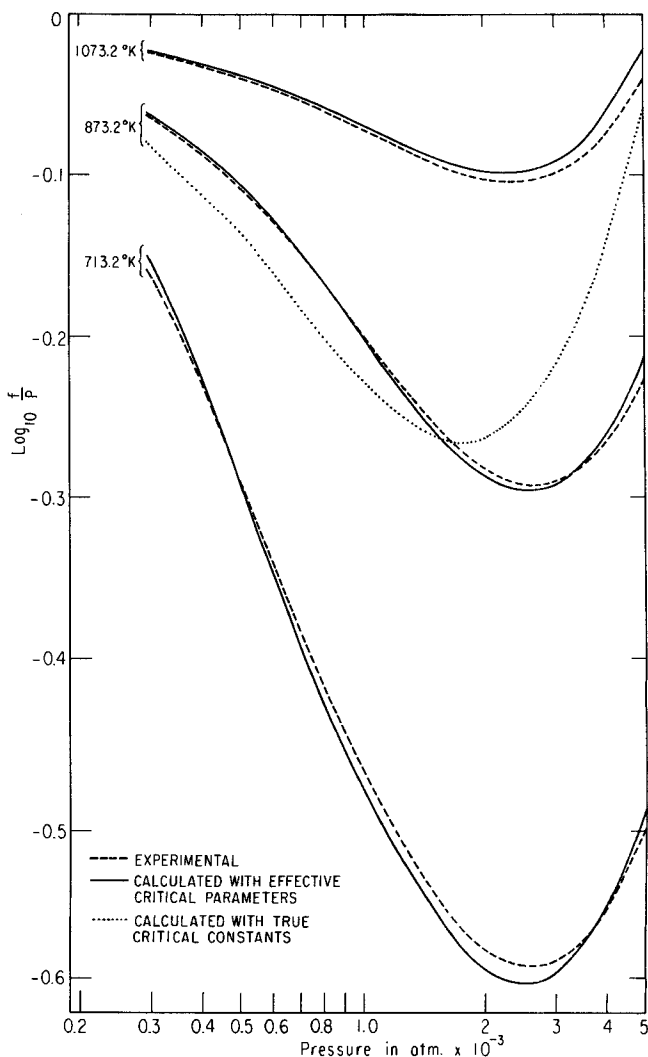


Fig. 8. Fugacity coefficients of water.

sociation, and chemical reactions. Further, at very high densities simple fluids may become metals. (See, for example, Alder, 1961; Brush, 1966; Ross, 1968.) However, for most practical chemical engineering applications that are likely to be of interest in the near future, these phenomena are probably not of major importance.

MIXTURES

Much attention has been given in recent years to the thermodynamic properties of simple mixtures at liquid densities. It has been shown, notably by Rowlinson (1969, pp. 328-333) and by Leland et al. (1968, 1969) that the van der Waals one-fluid or two-fluid model of mixtures gives good results. The limited experimental data for high pressures indicate that the two-fluid model gives better results than the one-fluid model (Breedveld, 1972).

For a binary mixture the two-fluid model is as follows: let Q stand for any extensive residual property (such as volume, entropy, Gibbs energy, etc.). We assume that

$$Q(\text{mixture}) = x_1 Q^{(1)} + x_2 Q^{(2)} \quad (3)$$

where x is the mole fraction. $Q^{(1)}$ is the quantity Q for a pure, hypothetical fluid whose critical constants are $V_c^{(1)}$, $T_c^{(1)}$, and $P_c^{(1)}$; similarly, $Q^{(2)}$ is the quantity Q for a pure, hypothetical fluid whose critical constants are $V_c^{(2)}$, $T_c^{(2)}$, and $P_c^{(2)}$.

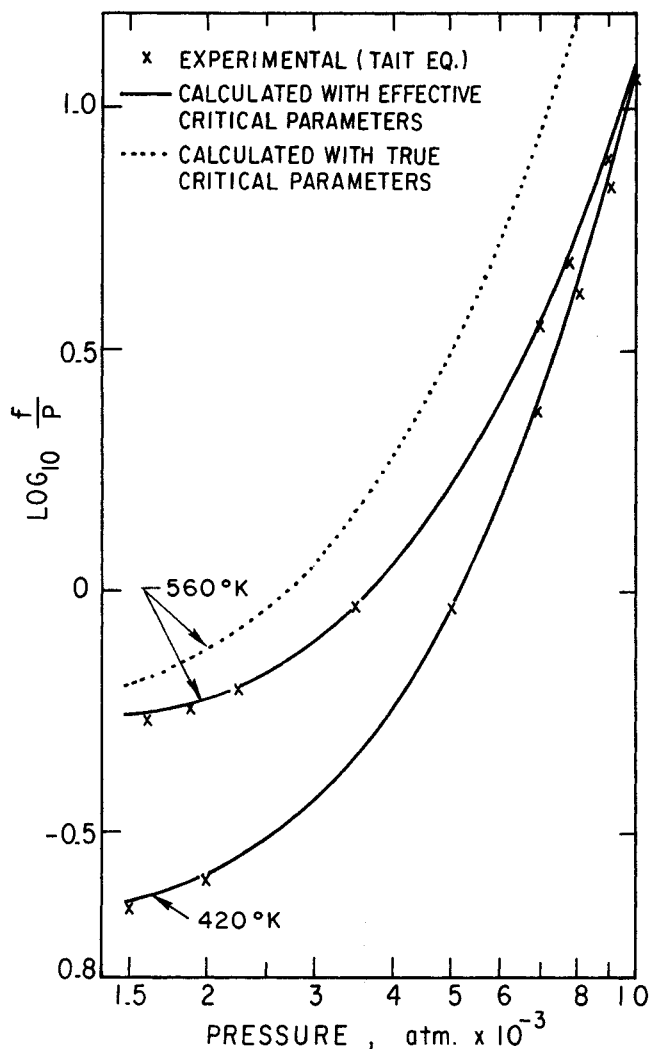


Fig. 9. Fugacity coefficients of ammonia

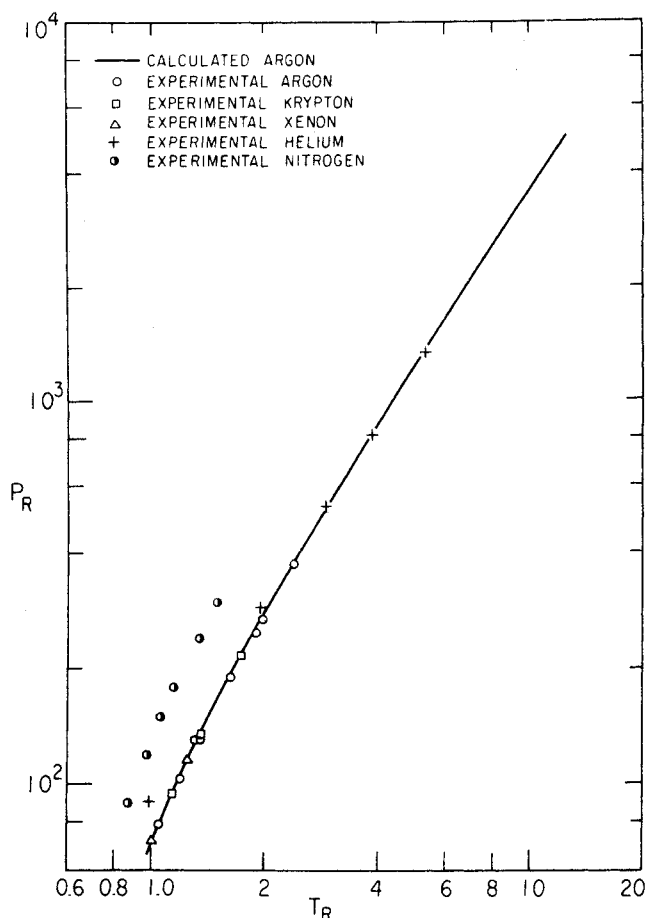


Fig. 10. Freezing points for very high pressures.

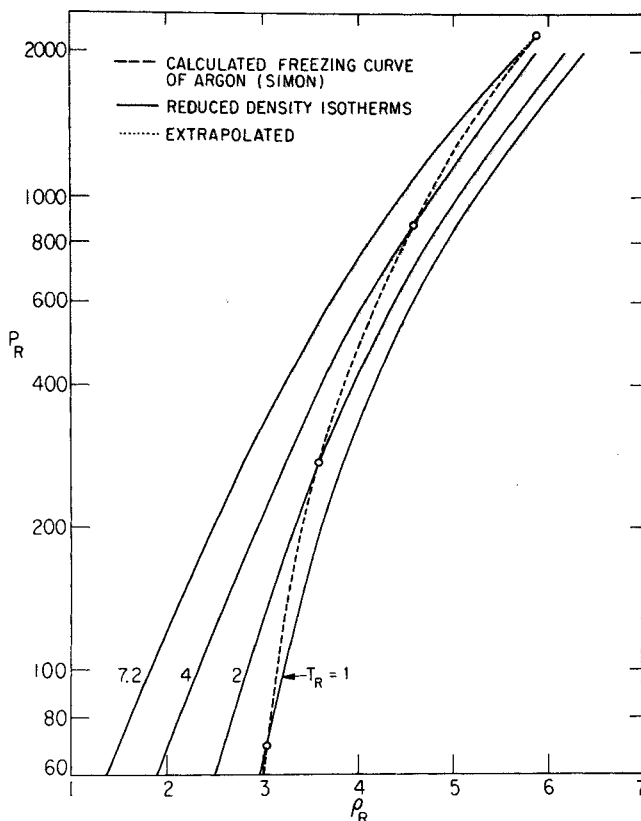


Fig. 11. Freezing curve of argon and reduced density isotherms.

The critical constants of these hypothetical fluids depend on the composition of the mixture:

$$V_c^{(1)} = x_1 V_{c1} + x_2 V_{c12} \quad (4)$$

$$V_c^{(2)} = x_2 V_{c2} + x_1 V_{c12}$$

$$V_c^{(1)} T_c^{(1)} = x_1 T_{c1} V_{c1} + x_2 T_{c12} V_{c12} \quad (5)$$

$$V_c^{(2)} T_c^{(2)} = x_2 T_{c2} V_{c2} + x_1 T_{c12} V_{c12}$$

$$P_c^{(1)} = 0.292 RT_c^{(1)} / V_c^{(1)} \quad (6)$$

$$P_c^{(2)} = 0.292 RT_c^{(2)} / V_c^{(2)}$$

The cross terms V_{c12} and T_{c12} are given by

$$V_{c12}^{1/3} = \frac{1}{2} (V_{c1}^{1/3} + V_{c2}^{1/3}) \quad (7)$$

$$T_{c12} = (T_{c1} T_{c2})^{1/2} (1 - k_{12}) \quad (8)$$

where k_{12} is a characteristic binary parameter, normally positive and (except for systems containing helium) small compared to unity. Estimates of k_{12} have been given by Chueh and Prausnitz, 1967 (see also Prausnitz, 1969, p. 157), and by Hiza and Duncan (1970) for a variety of

binary mixtures. For our calculations at high pressures these k_{12} factors had at times to be determined from the experimental results on the mixtures which were being studied.

For mixtures containing water, ammonia, or one of the quantum gases, Equations (4) through (8) must be modified, as illustrated in Appendix II.

Since few experimental PVT data have been reported for mixtures of supercritical fluids at very high pressures, it is not possible to make a thorough test of the two-fluid van der Waals model for mixtures under these conditions. However, for the few cases where a comparison can be made between theory and experiment agreement is good. Figure 12 shows compressibility factors ($Z = PV/RT$) for a mixture of nitrogen and methane, with $k_{12} = 0.046$ (Hiza and Duncan, 1970); calculated results compare well with experimental data of Blake et al. (1965). Figure 13 shows a similar comparison with data of Bennett and Dodge (1952) for mixtures of nitrogen and hydrogen with $k_{12} = 0.0$ (Hiza and Duncan, 1970) and Figure 14 with data of Canfield et al. (1965; see also Pfenning et al., 1965) for mixtures of nitrogen and helium. Finally, Figure 15 presents calculated and experimental enthalpies for nitrogen and helium; the experimental values were obtained from the PVT data of Canfield et al. (1965). For the nitrogen-helium mixtures, $k_{12} = 0.0$, as determined by us experimentally. (Calculations of enthalpies from the generalized chart require special care for quantum fluids where the effective critical constants depend on temperature. See Gunn et al., 1966.)

PARTIAL MISCIBILITY IN BINARY MIXTURES

Although predicted many years ago by van der Waals (1894), limited miscibility in binary supercritical fluid mixtures (gas-gas equilibria) was not observed experimentally until the 1940s (Krichevsky and Bolshakov, 1941; Tsiklis, 1952). Since then numerous experimental

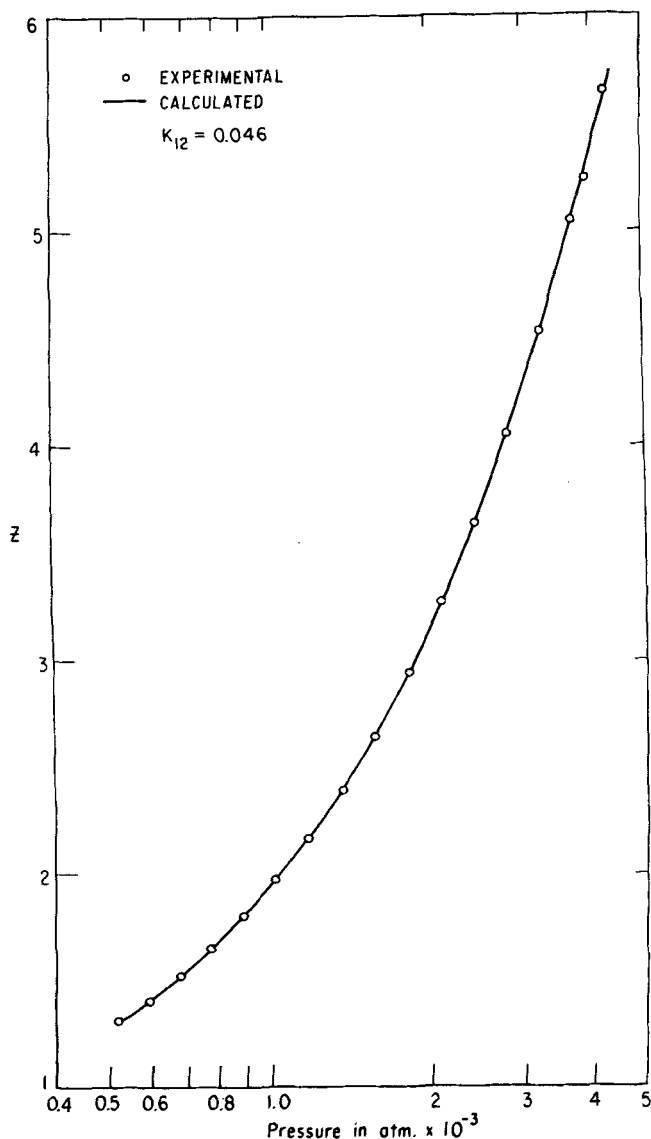


Fig. 12. Compressibility factors of an equimolar mixture of nitrogen and methane at 299.5°K.

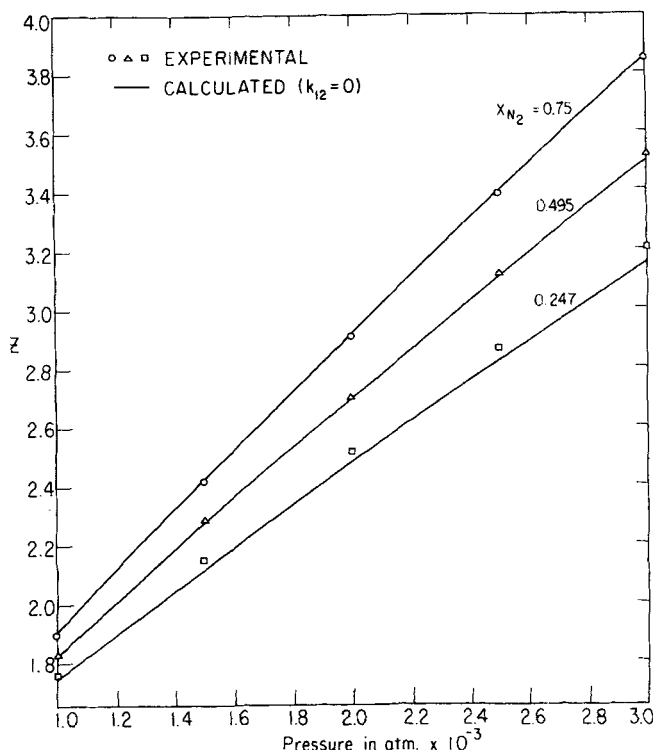


Fig. 13. Compressibility factors of nitrogen-hydrogen systems at 298.2°K.

studies have shown that at temperatures above the critical of the heavier component, two fluids may become partially immiscible at sufficiently high pressures (for example, Kaplan, 1968; Lindroos and Dodge, 1952; Schneider, 1970.)

At present, fluid-fluid separation at supercritical temperatures and pressures is primarily of theoretical interest,

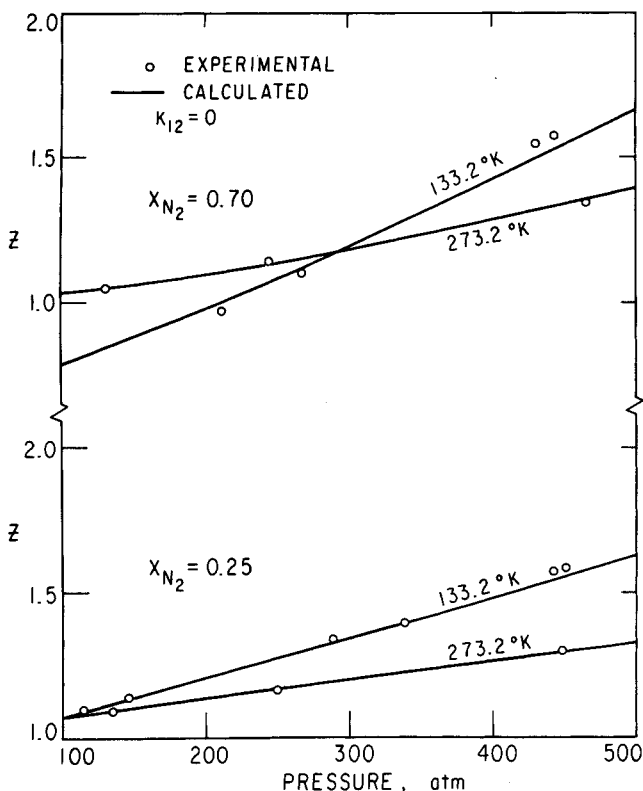


Fig. 14. Compressibility factors of helium-nitrogen systems.

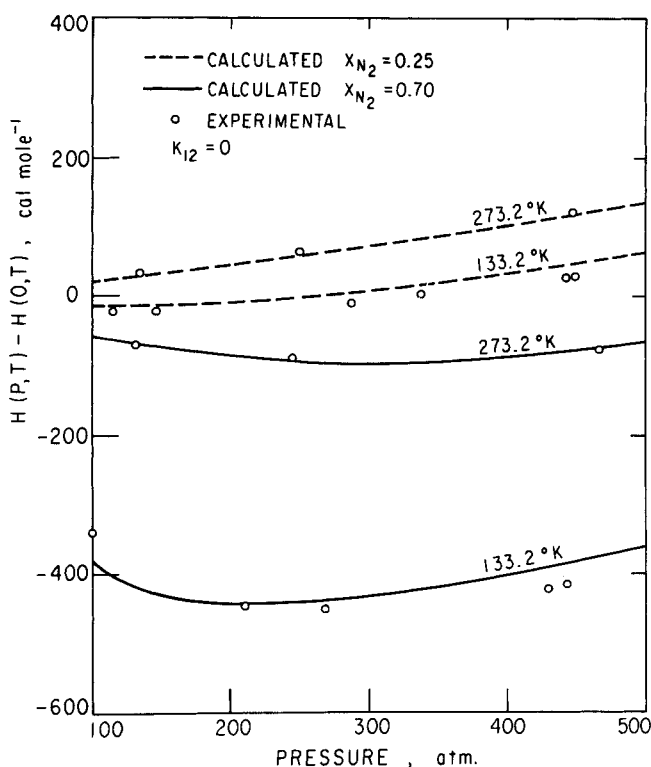


Fig. 15. Residual enthalpies for helium-nitrogen systems.

but in the future it may also become of practical importance; for example, in the case of chemical processes which for optimum efficiency have to be carried out at supercritical conditions, it is necessary to know whether one is dealing with a homogeneous or heterogeneous fluid phase.

High-pressure conditions in the earth's crust may cause fluid-fluid separation as well as those existing in the atmospheres of the heavier planets Jupiter and Saturn (Streett, 1969).

Several authors (for example, Kaplan, 1968; Kreglewski, 1957; Temkin, 1959; Tsiklis and Rott, 1957; Zandbergen et al., 1967) have discussed methods for predicting fluid-fluid separation of binary mixtures; notably Zandbergen et al. (1967) has used the single and three-liquid models of Prigogine (1957, Ch. 9) and Scott (1956) to estimate semiquantitatively the composition of the two coexisting phases of the xenon-helium system (De Swaan Arons and Diepen, 1966).

The two-fluid van der Waals model coupled with the generalized results shown in Figure 3 was used for a thermodynamic analysis of fluid-fluid equilibria. To this end we calculate ΔG^M , the molar Gibbs energy of mixing at constant pressure and temperature, from

$$\frac{\Delta G^M}{RT} = x_1 \left[\ln \left(\frac{f}{P} \right)^{(1)} - \ln \left(\frac{f}{P} \right)_1 + \ln x_1 \right] + x_2 \left[\ln \left(\frac{f}{P} \right)^{(2)} - \ln \left(\frac{f}{P} \right)_2 + \ln x_2 \right] \quad (9)^*$$

where $\ln(f/P)^{(i)}$ is found from Figure 3 using $T_c^{(i)}$ and $P_c^{(i)}$; similarly, $\ln(f/P)_i$ is found using T_{ci} and P_{ci} . The quantity $\Delta G^M/RT$ is plotted against x_1 ; if this plot has a point of inflection, two phases exist and their compositions can be found by constructing a common tangent as discussed elsewhere (Prausnitz, 1967, p. 234). This calculation is highly sensitive to small deviations in ΔG^M and the results, therefore, are necessarily approximate (Winnick and Powers, 1966).

At conditions close to phase separation, Equation (9) gives a ΔG^M which is more positive than observed; we ascribe this error to insufficient nonrandomness in the model given by Equations (3) to (9). Therefore, following Guggenheim, we added to Equation (9) a (negative) correction for nonrandomness based on the quasichemical approximation as described elsewhere (Hildebrand and Scott, 1950). To illustrate, Figure 16 shows $\Delta G^M/RT$ for the system xenon-helium at 325.7°K and 1000 atm, calculated first without, and then with, the nonrandomness correction; $k_{12} = 0.422$ (Hiza and Duncan, 1970). The uncorrected results indicate phase-splitting since a common tangent can be drawn to the dashed line. When the nonrandomness correction is included, we obtain the continuous line which indicates that only one phase exists at this temperature and pressure, in agreement with experiment (De Swaan Arons and Diepen, 1966).

Figure 17 shows a pressure-composition diagram for the system xenon-helium at 298.2°K. (The critical temperature of xenon is 289.8°K.) Also shown are experimental results of De Swaan Arons and Diepen (1966). At pressures below 420 atm helium and xenon are completely miscible, but at pressures above 420 atm two-fluid phases of different composition exist at equilibrium. The difference in composition increases as the pressure rises. The minimum pressure for phase separation depends on tem-

* Equation (9) is derived from Equation (3), as shown by Breedveld (1972).

perature; for many nonpolar systems the minimum pressure increases as the temperature is raised. For the xenon-helium system at 298.2°K we calculate a minimum pressure of 500 atm, and at 325.7°K we calculate 1100 atm in fair agreement with experiment.

Figure 18 compares calculated and observed critical lines for this system. We have included the critical line for the three-fluid model (Prausnitz, 1969, Section 7.10; Breedveld, 1972) with

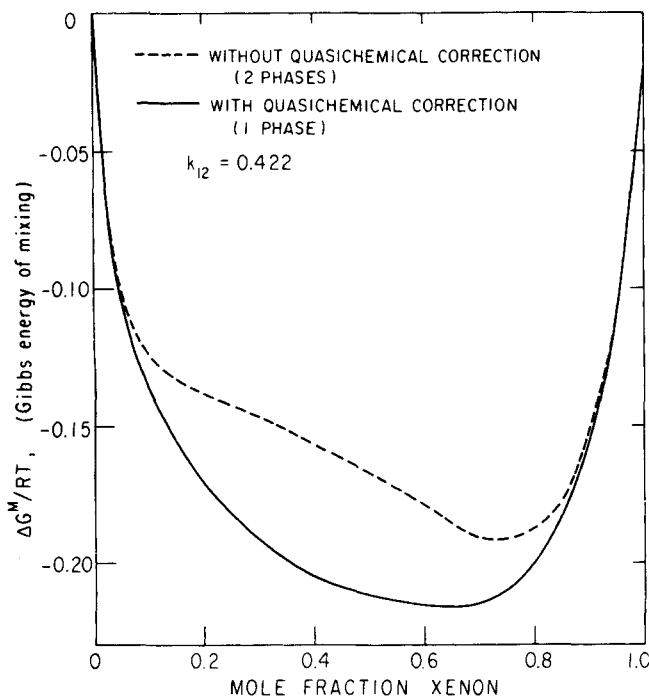


Fig. 16. Effect of the quasichemical correction to $\Delta G^M/RT$ for the xenon-helium systems (325.7°K, 1000 atm).

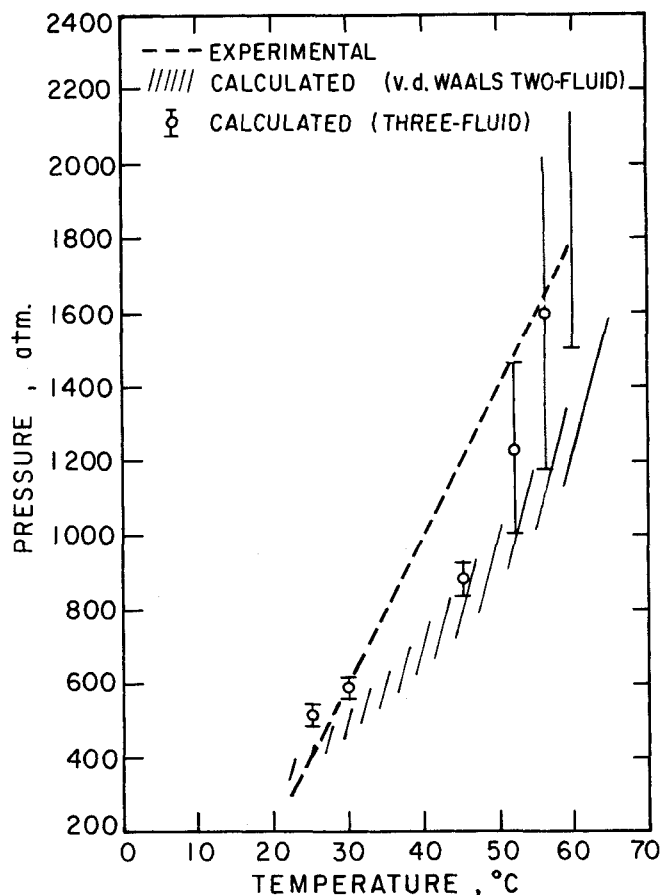


Fig. 18. Critical line for the xenon-helium system.

$$\frac{\Delta G^M}{RT} = A_{12}x_1x_2 + x_1 \ln x_1 + x_2 \ln x_2 \quad (10)$$

and

$$A_{12} = 2 \left\{ \ln \left(\frac{f}{P} \right)_{12} - \frac{1}{2} \left[\ln \left(\frac{f}{P} \right)_1 + \ln \left(\frac{f}{P} \right)_2 \right] \right\} \quad (11)$$

where $(f/P)_i$ is the fugacity coefficient of pure i and $(f/P)_{ij}$ the fugacity coefficient due to the interaction of pure components i and j . Equation (10) was presented by Zandbergen et al. (1967) in a somewhat different form. Phase instability exists when A_{12} has the value 2 or higher (Breedveld, 1972). In some cases, including this one, there appears to be a critical temperature beyond which no separation occurs. At this temperature and a corresponding pressure, A_{12} reaches the value of 2 as a maximum. For Xe-He the temperature and pressure are approximately 333°K and 2100 atm, respectively.

Figure 18 also shows the spread of pressures resulting from fluctuations in $\log_{10} (f/P)$ of $\pm 1\%$. The peculiar behavior of the three-fluid points, which show a spread markedly increasing with temperature, is due to the phenomenon discussed above. Such behavior is not shown by the two-fluid model, according to which phase separation persists to pressures well above 2100 atm, as suggested by the experimental results of De Swaan Arons and Diepen (1966). A similar discrepancy exists between predictions made with the three-fluid model and experimental results reported by Streett (1970) for the nitrogen-helium system. However, there are binary systems [for example, the argon-helium system (Streett and Hill, 1971)] where at the conditions of inter-

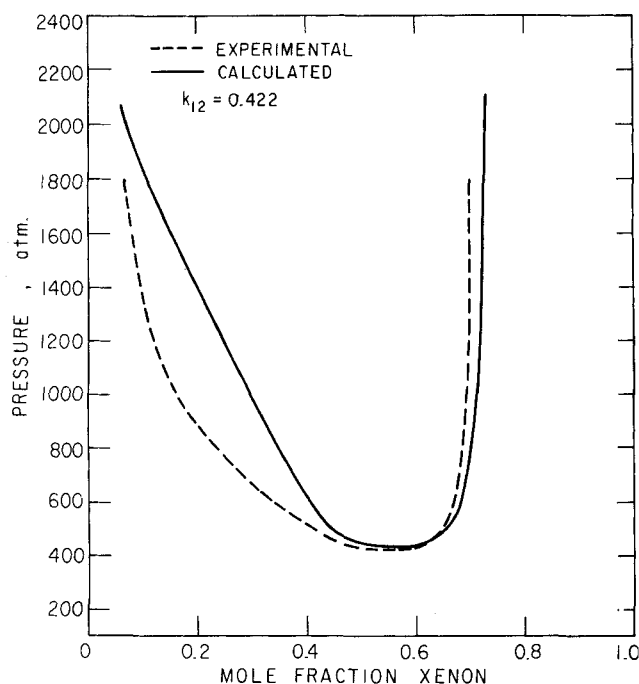


Fig. 17. Phase equilibria for the xenon-helium system at 298.2°K.

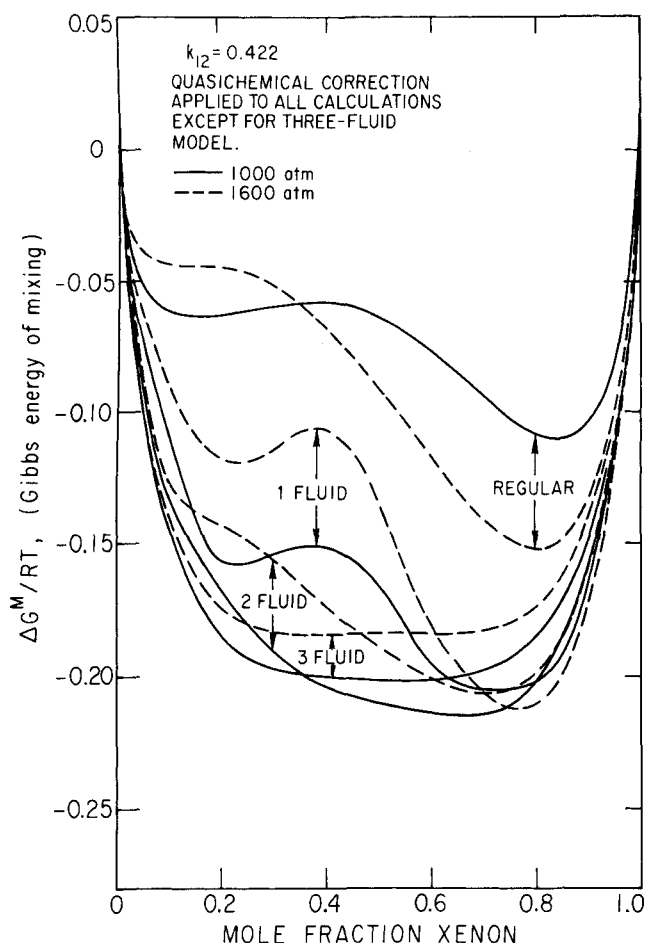


Fig. 19. Comparison of fluid models for the xenon-helium system (325.7°K, 1000 and 1600 atm).

est to us the three-fluid model does not exhibit this feature. As yet, we cannot explain this inconsistent performance of the three-fluid theory.

In Figure 19 plots of $\Delta G^M/RT$ versus the mole fraction x are compared for several fluid models at 325.7°K, 1000, and 1600 atm. In constructing the plot for the regular solution we could not fully follow the Scatchard-Hildebrand theory (Hildebrand et al., 1970) because of negative cohesive-energy densities for He. Consequently, the somewhat modified method, as discussed in Appendix I, was used.

Figure 19 indicates the usefulness of the generalized tables and clearly differentiates between several fluid models. For the xenon-helium system, which at this temperature shows incipient phase separation at about 1500 atm (De Swaan Arons and Diepen, 1966), it reveals that the two- and three-fluid theory yield results closest to experiment. Those obtained from the one-fluid theory and the regular solution theory deviate most.

Figure 20 gives a phase diagram for the system ethane-water at 653.2°K with $k_{12} = 0.12$, as determined experimentally. (The critical temperature of water is 647.4°K.) Calculated results using the two-fluid model compare semiquantitatively with experimental data of Danneil et al. (1967).

PARTIAL MISCIBILITY IN TERNARY MIXTURES

The formulas used for calculating thermodynamic properties of binary mixtures are readily extended to multicomponent mixtures (Breedveld, 1972). Unfortun-

nately, suitable experimental data for ternary systems are very scarce. Those closest to our requirements refer to the ammonia-nitrogen-hydrogen system (Krichevsky and Tsiklis, 1943), who report that two phases exist at 373 to 378°K and pressures of about 2200 to 5000 atm. These conditions differ widely from those currently applied in the ammonia synthesis industry (reactor temperature about 773°K, reactor pressure about 300 atm), and as far as the temperatures are concerned are outside the applicability range of our fugacity and density tables; a rough extrapolation of the figures shown in Table 5 results in an effective $T_R^* \approx 0.87$. (This also applies to the ammonia-methane-nitrogen system discussed by Tsiklis, 1951.)

Since it may become feasible and worthwhile to calculate ternary equilibria in the near future, a brief description follows of a method for calculating phase instability. It consists of first calculating the molar excess Gibbs energy at constant temperature and pressure of each of the three binaries which comprise the ternary. This calculation is shown elsewhere (Breedveld, 1972) for several fluid theories. Where necessary, as, for example, for the van der Waals two-fluid theory, the quasichemical non-randomness correction is included. For each binary the excess Gibbs energy is fitted to a semi-empirical equation [for example, the van Laar, Margules or NRTL equation, (Renon et al., 1971)] and these equations can then be used to predict the excess Gibbs energy of the ternary system (Prausnitz, 1969, Ch. 6). Appropriate differentiation gives the activity coefficients whereafter one can, for example, proceed according to Renon et al. (1971) to calculate the phase behavior of the ternary mixture.

ACKNOWLEDGMENT

The authors are grateful to the National Science Foundation for financial support and to the University of California Computer Center for the use of its facilities.

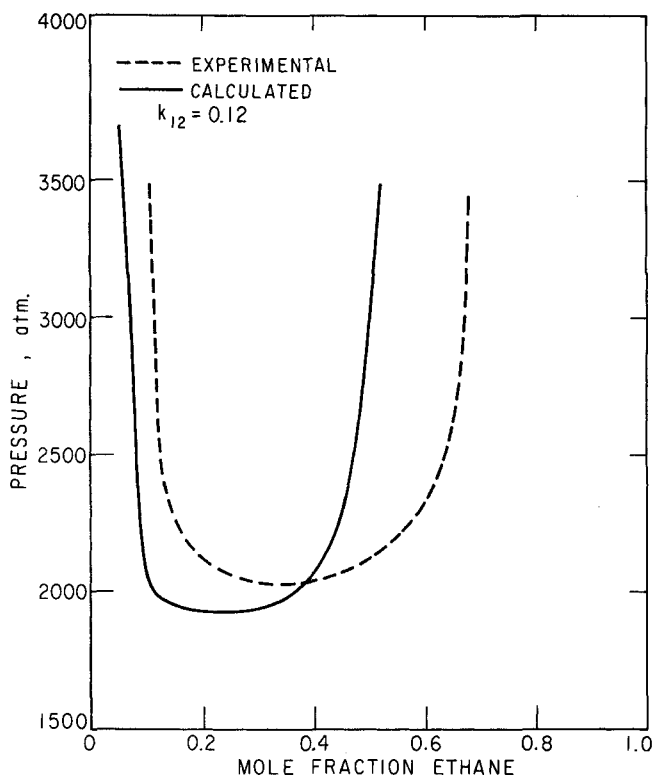


Fig. 20. Phase equilibrium for the water-ethane system at 653.2°K.

NOTATION

A	= interaction parameter for mixtures
C_1, C_2, C_3	= constants in expressions for quantum gases, deg
c	= cohesive energy density, cal cm ⁻³
d	= constant in Simon equation
f	= fugacity, atm
G	= molar Gibbs energy, cal mol ⁻¹
H	= molar enthalpy, cal mol ⁻¹
\ln	= natural logarithm
\log_{10}	= LOG = logarithm to the base of 10
k	= correction to geometric mean (subscripted)
k	= Boltzmann constant, erg deg ⁻¹ molecule ⁻¹
M	= molecular weight
N_{AV}	= Avogadro's number, molecules mol ⁻¹
P	= pressure, atm
Q	= residual property = difference of real and ideal gas value of property at P and T
R	= gas constant, cm ³ atm deg ⁻¹ mol ⁻¹ or cal deg ⁻¹ mol ⁻¹
r	= intermolecular separation, Å
T	= temperature, deg Kelvin
U	= internal energy, cal mol ⁻¹
V	= molar volume cm ³ mol ⁻¹
x	= mole fraction
Z	= compressibility factor
(O, T)	= zero atm, $T^\circ K$
(P, T)	= P atm, $T^\circ K$
U, H, G	= configurational properties unless otherwise stated

Greek Letters

α	= polarizability, cm ³ × 10 ²⁴
$\bar{\Gamma}$	= average intermolecular potential, erg
Δ	= difference
δ	= solubility parameter, cal ^{1/2} cm ^{-3/2}
ϵ	= characteristic energy parameter of a Lennard-Jones pair potential, erg
μ	= dipole moment, Debye units
ρ	= density, mol cm ⁻³
σ	= collision diameter, equal to intermolecular distance at zero Lennard-Jones potential, Å
Φ	= volume fraction using molar volumes of components
ω	= Pitzer acentric factor

Superscripts

E	= excess property
$*$	= effective property
(1), (i), (j)	= hypothetical fluid components of a mixture
M	= due to mixing
0	= characteristic effective property at very high temperature or in absence of interaction due to dipoles

Subscripts

c	= critical property
i, j, k	= individual molecules or components in mixture
M	= of mixture
m	= melting point in Simon equation
0	= constant in Simon equation
R	= reduced property

LITERATURE CITED

- Alder, B. J., in "Progress in Very High Pressure Research," p. 152, *Proc. Intern. Conf.*, Lake George, New York (1961).
- Bae, J. H., and T. M. Reed, "Estimation of Properties of Dilute Polar Gases from a Potential Energy Function," *Ind. Eng. Chem. Fundamentals*, **6**, 67 (1967).
- Bennett, C. O., and B. F. Dodge, "Compressibilities of Mixtures of Hydrogen and Nitrogen above 1000 Atmospheres," *Ind. Eng. Chem.*, **44**, 180 (1952).
- Blake, A. G., B. S. Bretton, and B. F. Dodge, "The Volumetric Behavior of Methane, Nitrogen, and Some Mixtures at Pressures up to 5000 Atmospheres," *AIChE-I. Chem. Eng., Symp. Ser. No. 2*, p. 1, Inst. Chem. Engrs., London (1965).
- Breedveld, G. J. F., Ph.D. dissertation, Univ. California, Berkeley (1972).
- Bridgman, P. W., "The Compressibility of Five Gases to High Pressures," *Proc. Amer. Acad. Arts Sci.*, **59**, 173 (1924).
- Brush, S. G., "Theories of the Equation of State of Matter at High Pressures and Temperatures," in *Progress in High Temperature Physics and Chemistry*, Vol. 1, 1, C. A. Rouse (Ed.), Pergamon Press, London (1966).
- Buchmann, E., "Helium Isothermen bei Tiefen Temperaturen und Hohen Drücken," *Z. Phys. Chem., Abt. A*, **163**, 461 (1933).
- Burnham, C. W., J. J. Holloway, and N. F. Davis, "Thermodynamic Properties of Water to 1,000°C and 10,000 Bars," Special Paper No. 132, The Geol. Soc. America, Boulder, Colorado (1969).
- Canfield, F. B., T. W. Leland, and R. Kobayashi, "Compressibility Factors for Helium-Nitrogen Mixtures," *J. Chem. Eng. Data*, **10**, 92 (1965).
- Chueh, P. L., and J. M. Prausnitz, "Vapor-Liquid Equilibria at High Pressures. Vapor-Phase Fugacity Coefficients in Non-polar and Quantum-Gas Mixtures," *Ind. Eng. Chem. Fundamentals*, **6**, 492 (1967).
- Cook, D., and J. S. Rowlinson, "Deviations from the Principle of Corresponding States," *Proc. Roy. Soc., Ser. A*, **219**, 405 (1953).
- Danon, F., and I. Amdur, "Averaged Potentials and the Viscosity of Dilute Polar Gases," *J. Phys. Chem.*, **50**, 4178 (1969).
- Danneil, A., A. Tödheide, and E. U. Franck, "Verdampfungs-gleichgewichte und kritische Kurven in den Systemen Athan/Wasser und n-Butan/Wasser bei hohen Drücken," *Chem. Ing. Tech.*, **13**, 816 (1967).
- De Swaan Arons, J., and G. A. M. Diepen, "Gas-Gas Equilibria," *J. Chem. Phys.*, **44**, 2322 (1966).
- Din, F., *Thermodynamic Functions of Gases*, Butterworths, London Vol. 1, (1956), Vol. 2 (1956), Vol. 3 (1961).
- Dodge, B. F., *Chemical Engineering Thermodynamics*, Chap. 5 and 6, McGraw-Hill, New York (1944).
- Goodwin, R. D., D. E. Diller, H. M. Roder, and L. A. Weber, "Pressure-Density-Temperature Relations of Fluid Para Hydrogen from 15 to 100°K at Pressures to 350 Atmospheres," *J. Res. Nat. Bur. Stand., A (Phys. & Chem.)*, **67**, 173 (1962).
- Gonikberg, M. G., "Chemical Equilibria and Reaction Rates at High Pressures," trans. from Russian, Nat. Sci. Foundation, Washington, D.C. (1960).
- Gosman, A. L., R. D. McCarty, and J. G. Hust, "Thermodynamic Properties of Argon from the Triple Point to 300°K at Pressures to 1000 Atmospheres," *Nat. Bur. Stand., NSRDS-NBS*, **27** (1969).
- Gunn, R. D., P. L. Chueh, and J. M. Prausnitz, "Prediction of Thermodynamic Properties of Dense Gas Mixtures Containing One or More of the Quantum Gases," *AIChE J.*, **12**, 937 (1966).
- Harrison, E. F., "Intermolecular-Force Effects on the Thermodynamic Properties of Helium with Application," *AIAA J.*, **2**, 1854 (1964).
- Hildebrand, J. H., and R. L. Scott, "The Solubility of Non-electrolytes," Ch. 8, 3rd Ed. (1950), reprinted Dover, New York (1964).
- Hildebrand, J. H., J. M. Prausnitz, and L. S. Scott, *Regular and Related Solutions*, Van Nostrand Reinhold, New York (1970).
- Hilsenrath, J., (ed.), *Tables of Thermodynamic and Transport Properties of Air, Argon, Carbon Dioxide, Carbon Monoxide, Hydrogen, Nitrogen, Oxygen and Steam*, Pergamon Press, London, Paris (1960).
- Hirschfelder, J. O., C. F. Curtis, and R. B. Bird, *Molecular Theory of Gases and Liquids*, p. 987, Wiley, New York and Chapman & Hall, London (1967).

sure. The volume fractions Φ_1 and Φ_2 are defined by

$$\Phi_1 = \frac{x_1 V_1}{x_1 V_1 + x_2 V_2}; \quad \Phi_2 = \frac{x_2 V_2}{x_1 V_1 + x_2 V_2}, \quad (\text{I-2})$$

and the cohesive energy density c by

$$c = \frac{U(0, T) - U(P, T)}{V} \quad (\text{I-3})$$

For liquids ($T_R < 1$), c is a positive quantity; the positive square root of c is the well-known solubility parameter. As shown in Figure 6, for supercritical fluids c is positive at lower pressures and temperatures but becomes increasingly negative as these rise. For the pure fluids, c_{11} and c_{22} are readily found from Equation (I-3) and the correlations shown in Figures 1 and 4 (or 5). The cross-term c_{12} is found from

$$\begin{aligned} \frac{c_{12}}{RT} &= \frac{H_{12}(0, T) - H_{12}(P, T) - RT \left(1 - \frac{PV_{12}}{RT} \right)}{V_{12}RT} \\ &= \frac{1}{V_{12}} \left[\left(\frac{\Delta H}{RT_c} \right)_{12} \cdot \frac{1}{T_{R12}} - 1 + \frac{PV_{12}}{RT} \right] \quad (\text{I-4}) \end{aligned}$$

To find V_{12} and $(\Delta H/RT_c)_{12}$ we again use Figures 1 and 4 (or 5). The required critical constants V_{c12} , T_{c12} and P_{c12} are given by Equations (7) and (8) and

$$P_{c12} = \frac{0.292 RT_{c12}}{V_{c12}} \quad (\text{I-5})$$

APPENDIX II. POLAR FLUIDS

From the model presented by Danon and Amdur (1969), and Cook and Rowlinson (1953), one can derive for the average interaction potential \bar{r} [including second-order contributions of dipole-dipole interactions and spherical polarizability (Bae and Reed, 1967)],

$$\begin{aligned} \bar{r} &= 4\epsilon^0 \left[\left(\frac{\sigma^0}{r} \right)^{12} - \left(\frac{\sigma^0}{r} \right)^6 \right] - \frac{\mu^4}{3r^6 kT} \\ &\quad - \frac{2\alpha\mu^2}{r^6} + \frac{7\mu^8}{450r^{12}(kT)^3} \quad (\text{II-1}) \end{aligned}$$

The fluid, whose potential is given by Equation (II-1), is supposed to be conformal (Rowlinson, 1969, p. 266) with the reference substance of the generalized tables.

We define temperature-dependent effective parameters ϵ^* and σ^* by

$$\bar{r}^* = 4\epsilon^* \left[\left(\frac{\sigma^*}{r} \right)^{12} - \left(\frac{\sigma^*}{r} \right)^6 \right] \quad (\text{II-2})$$

where \bar{r}^* is the average, temperature-dependent interaction potential.

For a Lennard-Jones (6, 12) potential and for effectively spherical molecules, the critical constants P_c , V_c , and T_c are related to the force constants ϵ and σ by (Rowlinson, 1969, p. 269)

$$T_c = 1.25 \epsilon/k \quad (\text{II-3})$$

$$V_c = 3.14 N_{AV} \sigma^3 \quad (\text{II-4})$$

$$P_c = \frac{0.292 RT_c}{V_c} \quad (\text{II-5})$$

By equating the coefficients of r^{-12} and r^{-6} in Equations (II-1) and (II-2) and substituting the critical constants from Equations (II-3) and (II-4), we obtain

$$T_c^* = T_c^0 \frac{(1+A)^2}{(1+B)} \left[1 + \frac{3.23 \times 10^4 \alpha \mu^2 (1+A) + D}{T_c^0 (V_c^0)^2 (1+A)^2} \right] \quad (\text{II-6})$$

$$V_c^* = V_c^0 \left(\frac{1+B}{1+A+C} \right)^{1/2} \quad (\text{II-7})$$

where

$$A = 1.95 \times 10^7 \frac{\mu^4}{T_c^0 (V_c^0)^2 T} \quad (\text{II-8})$$

$$B = 1.72 \times 10^{14} \frac{\mu^8}{T_c^0 (V_c^0)^4 T^3} \quad (\text{II-9})$$

$$C = 1.62 \times 10^4 \times \frac{\alpha \mu^2}{T_c^0 (V_c^0)^2} \quad (\text{II-10})$$

$$D = 2.62 \times 10^8 \frac{\alpha^2 \mu^4}{T_c^0 (V_c^0)^2} \quad (\text{II-11})$$

P_c^* and P_c^0 are obtained from the corresponding critical volumes and temperatures according to Equation (II-5).

P_c^* , T_c^* , and V_c^* are effective temperature-dependent critical properties of a hypothetical fluid representing the original polar fluid at the desired pressures and temperatures. It also is conformal with the reference fluid of the generalized tables.

The values of above parameters are obtained by fitting experimental data to the generalized tables (Breedveld, 1972).

Mixtures of Polar and Nonpolar Fluids

The average Lennard-Jones (6, 12) potential between a nonpolar molecule 1 and a polar molecule 2 is (Hirschfelder, 1967),

$$\bar{r} = 4\epsilon_{12}^0 \left[\left(\frac{\sigma_{12}^0}{r} \right)^{12} - \left(\frac{\sigma_{12}^0}{r} \right)^6 \right] - \frac{\alpha_1 \mu_2^2}{r^6} \quad (\text{II-12})$$

where ϵ_{12}^0 and σ_{12}^0 are the interaction parameters as they would have been if both fluids had been nonpolar. As shown above for a binary mixture of polar molecules, Equation (II-12) can be transformed into the Lennard-Jones (6, 12) form with the effective parameters ϵ_{12}^* and σ_{12}^* given by

$$\epsilon_{12}^* = \epsilon_{12}^0 \left[1 + \frac{\alpha_1 \mu_2^2}{4\epsilon_{12}^0 (\sigma_{12}^0)^6} \right]^2 \quad (\text{II-13})$$

$$\sigma_{12}^* = \sigma_{12}^0 \left[1 + \frac{\alpha_1 \mu_2^2}{4\epsilon_{12}^0 (\sigma_{12}^0)^6} \right]^{-1/6} \quad (\text{II-14})$$

After substituting the critical temperature and volume [Equations (II-3) and (II-4)] for the molecular force constants and introducing the binary correction term k_{12} for the geometric mean of the critical temperature, we obtain

$$T_{c12}^* = (T_{c1}^0 T_{c2}^0)^{1/2} (1 - k_{12}) (1 + \text{IND})^2 \quad (\text{II-15})$$

$$V_{c12}^* = \frac{\left[\frac{1}{2} \{ (V_{c1}^0)^{1/3} + (V_{c2}^0)^{1/3} \} \right]^3}{(1 + \text{IND})^{1/2}} \quad (\text{II-16})$$

where

IND =

$$\frac{8.07 \times 10^3 \alpha_1 \mu_2^2}{(T_{c1}^0 T_{c2}^0)^{1/2} (1 - k_{12}) \left[\frac{1}{2} \{ (V_{c1}^0)^{1/3} + (V_{c2}^0)^{1/3} \} \right]^6} \quad (\text{II-17})$$

and where T_{c2}^0 and V_{c2}^0 follow from Equations (II-6) and (II-7).

Also

$$P_{c12}^* = \frac{0.292 RT_{c12}^*}{V_{c12}^*} \quad (\text{II-18})$$

For calculations employing, for example, the van der Waals two-fluid model, the effective critical parameters T_{c2}^* , V_{c2}^* , T_{c12}^* , V_{c12}^* instead of T_{c2}^0 , V_{c2}^0 , T_{c12}^0 and V_{c12}^0 respectively, must be used in Equations (5) to (7).

Manuscript received December 28, 1972; revision received March 13 and accepted March 16, 1973.